

Three-body system of $\pi\pi\Sigma_c$

Bingwei Long^{1,*}

¹*Center for Theoretical Physics, Department of Physics,
Sichuan University, 29 Wang-Jiang Road, Chengdu, Sichuan 610064, China*

(Dated: September 29, 2016)

Abstract

The existence of near-threshold charmed baryon $\Lambda_c^+(2595)$ implies the pion and the lightest, isospin-1 charmed baryon Σ_c interact very strongly at extremely low energies. Using the two-flavor version of heavy hadron chiral perturbation theory, I explore the direct consequences of this strong force by investigating whether the Σ_c can trap two very soft pions to form any visible hadronic states. The answer is positive. It is found without tuning any free parameters or ultraviolet cutoff that the state in question, with quantum numbers $I(J^P) = 1(\frac{1}{2}^+)$, presents itself as a resonance pole only a few MeVs away from the $\pi\pi\Sigma_c$ threshold. Subleading corrections are estimated with power-counting arguments, and the smallness of pion momenta is found to facilitate the reliability of the analysis. Because of its proximity in mass, this excited Σ_c resonance is speculated to be related to the broad resonance labeled as $\Lambda_c^+(2765)$.

*Electronic address: bingwei@scu.edu.cn

If hadronic states are resonances or bound states close to the threshold of two or more lighter hadrons, they very likely attract interests by encouraging us to draw analogies with molecules. We may be able to understand their structure by, often nonrelativistic, few-body dynamics of constituent particles without having to disentangle the complicated details of quantum chromodynamics (QCD). It will be even more interesting if some of the constituents are pseudo-Goldstone bosons, like pions, because the approximate chiral symmetry of QCD restricts how they interact with other hadrons, which is conveniently formulated in chiral perturbation theory (ChPT). Negative-parity, isoscalar, and spin-1/2 charmed baryon $\Lambda_c^+(2595)$ is such a state, situated $\delta \equiv \Delta - m_\pi \simeq 1$ MeV above the $\pi\Sigma_c$ threshold, where Σ_c is the lightest isospin-1 charmed baryon, with a mass smaller than $\Lambda_c^+(2595)$ by $\Delta \simeq 139$ MeV [1]. Σ_c can decay into the ground-state charmed baryon Λ_c^+ but the width $\simeq 2$ MeV is relatively small. So the Σ_c is approximated here as a stable state.

Due to its quantum numbers, $\Lambda_c^+(2595)$, denoted by Λ_c^* from now on, couples in the S wave to the isoscalar channel of $\pi\Sigma_c$. The closeness of Λ_c^* to the $\pi\Sigma_c$ threshold indicates that the resonant, S -wave interaction of $\pi\Sigma_c$ is incredibly strong at very low energies that are characterized by the size of the pion three-momentum around the Λ_c^* resonance, $Q \sim \sqrt{2\delta m_\pi} \simeq 20$ MeV. I explore the direct consequences of this strong low-energy attraction between the pion and the Σ_c , by investigating whether the Σ_c can trap multiple pions to form heavier hadronic molecules. As the first step along this line of research, I study the three-body system of $\pi\pi\Sigma_c$ with the quantum numbers $I(J^P) = 1(\frac{1}{2}^+)$, which is compatible with the isoscalar, S -wave $\pi\Sigma_c$ interaction. It is found without any free parameters at leading order (LO) that there exists a Σ_c resonance near the $\pi\pi\Sigma_c$ threshold, with both real and imaginary parts of its pole position at most a few MeVs away from the threshold.

The low-energy character of the $\pi\Sigma_c$ interaction makes it possible to focus on the small phase space around the $\pi\pi\Sigma_c$ threshold in which all three particles have momenta comparable to Q . Since the particles are almost on-shell and relatively stable, the nonrelativistic few-body dynamics is adequate and the states far away in energy from the threshold can be “integrated out”. In order to exploit systematically the smallness of Q , I use a specialized version of heavy hadron chiral perturbation theory (HHChPT) [2–5] that includes only light flavors of u and d .

The interactions between two pions must be weak because they are proportional to Q^2 or m_π^2 , owing to the spontaneous breaking of chiral symmetry. However, the $\pi\pi\Sigma_c$ system

is not a straightforward problem of weakly interacting bosons trapped in a potential. The resonant nature of $\pi\Sigma_c$ interaction, at least in the ChPT framework, inevitably leads to an energy-dependent $\pi\Sigma_c$ potential, which invalidates separation of the pions' coordinates in the Schrödinger equation. This forces us to be content with numerical solutions.

For the time being, only Σ_c , Λ_c^* and pions are relevant degrees of freedom, so we consider the usual heavy-baryon chiral Lagrangian without heavy quark symmetry manifestly incorporated. The relevant leading terms [6] are

$$\begin{aligned}\mathcal{L} = & i\Sigma_a^\dagger \dot{\Sigma}_a + \frac{i}{f_\pi^2} \Sigma_a^\dagger (\pi_a \dot{\pi}_b - \pi_b \dot{\pi}_a) \Sigma_b \\ & + \Psi^\dagger (i\partial_0 - \Delta) \Psi + \frac{h}{\sqrt{3}f_\pi} (\Sigma_a^\dagger \dot{\pi}_a \Psi + \text{H.c.}) \\ & + \left(\frac{m_\pi^2}{2} \pi^2 - \dot{\pi}^2 \right) \frac{\pi^2}{4f_\pi^2} + \dots\end{aligned}\tag{1}$$

Here Ψ (Σ) is the field that annihilates Λ_c^* (Σ_c). The pion decay constant $f_\pi = 92.4$ MeV, and the $\pi\Sigma_c\Lambda_c^*$ transition coupling $h^2 = 3/2 h_2^2$, where h_2 is the counterpart of h in the HHChPT Lagrangian [5]. At LO, the transition vertex is approximately proportional to m_π because the pion momenta are very small. The second term of the first line is the Weinberg-Tomazawa term for the Σ_c , and the third line is the leading S -wave pion-pion interaction. I use throughout the paper the heavy-baryon notation for baryon energies, which have the mass of Σ_c subtracted.

The two-body interaction of $\pi\Sigma_c$ is can be encapsulated in the dressed Λ_c^* propagator, shown in Fig. 1,

$$iD(p) = \frac{i}{(p_0 - m_\pi) - \delta - \epsilon h^2 \sqrt{2(m_\pi - p_0)m_\pi}},\tag{2}$$

where, besides δ , $\epsilon \equiv m_\pi^2/4\pi f_\pi^2 = 0.18$ is the other small parameter to be exploited here. Since we are only interested in very low energies at which $\pi\Sigma_c$ interaction is resonant, we can consider for power-counting purposes that $|p_0 - m_\pi| \sim \delta$. The dressing is necessary when each term of the denominator in Eq. (2) is of the same size. It immediately follows that $\delta \sim Q^2/m_\pi \sim \epsilon^2 m_\pi$, where we have used $h = \mathcal{O}(1)$. It can be numerically verified that δ and $\epsilon^2 m_\pi$ are indeed of the same order of magnitude.

Attaching $\pi\Sigma_c\Lambda_c^*$ vertexes to the dressed Λ_c^* propagator, we obtain the $\pi\Sigma_c$ elastic scattering amplitude and extract the scattering length and effective range as follows [6],

$$-1/a = \frac{\delta}{\epsilon h^2}, \quad r = -(\epsilon h^2 m_\pi)^{-1}.\tag{3}$$

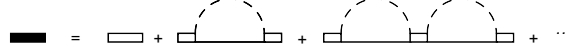


FIG. 1: The dressed Λ_c^* propagator. The double, solid, and dashed lines represent propagation of a Λ_c^* , a Σ_c , and a pion, respectively.

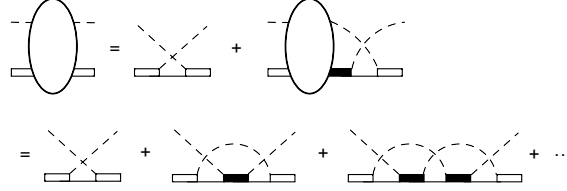


FIG. 2: Resummation of Σ_c -exchanges in $\pi\Lambda_c^*$ scattering.

Since there is not any physical difference between the Ψ field and composite operator $\pi_b \Sigma_b$, any correlation functions of the form $\langle 0 | \pi_a \Psi \pi_a \Psi^\dagger | 0 \rangle$ can be used to search for potential states associated with $\pi\pi\Sigma_c$. I choose to study the pole structure of the $\pi\Lambda_c^*$ scattering amplitude, represented by the blob in Fig. 2. In the center-of-mass (CM) frame, the pion has incoming (outgoing) four-momentum $(k_0 + m_\pi, \vec{k})$ $[(q_0 + m_\pi, \vec{q})]$ and the baryon has incoming (outgoing) four-momentum $(E_\Lambda + m_\pi, -\vec{k})$ $[(E - q_0 + m_\pi, -\vec{q})]$, where E_Λ is the energy of Λ_c^* . In my notation the CM energy $\sqrt{s} = E + 2m_\pi + M_{\Sigma_c}$, and $E = \vec{q}^2/2m_\pi + E_\Lambda$ when the external pions are on-shell, but the external Λ_c^* are not necessarily so.

We can break up any $\pi\Lambda_c^*$ scattering diagrams into two parts: (1) $\pi\Lambda_c^*$ potentials, diagrams that are still connected after a pion and a Λ_c^* internal lines are cut, and (2) propagation of $\pi\Lambda_c^*$ with the dressed Λ_c^* propagator. The dominant $\pi\Lambda_c^*$ potential is the u -channel Σ_c -exchange. Illustrated in the second line of Fig. 2 are Σ_c exchanges connected by $\pi\Lambda_c^*$ propagators. Using power-counting language, I argue as follow that these diagrams must be resummed.

The pion's kinetic energy is $\sim Q^2/m_\pi$, so is the energy following through baryon propagators. Therefore, the Σ_c propagator contributes a factor of $(Q^2/m_\pi)^{-1}$. With the $\pi\Sigma_c\Lambda_c^*$ vertex $\sim (m_\pi/f_\pi)$, the LO potential is then counted as

$$\frac{m_\pi}{f_\pi} \frac{1}{Q^2/m_\pi} \frac{m_\pi}{f_\pi} \sim \frac{m_\pi^3}{f_\pi^2 Q^2}. \quad (4)$$

The propagation of $\pi\Lambda_c^*$ intermediate states consists of a pion propagator contributing a factor of $1/Q^2$, a dressed Λ_c^* propagator $\sim (Q^2/m_\pi)^{-1}$, and the loop integration $\int dl_0 d^3l \sim (Q^2/m_\pi)Q^3$. The numerical factor associated with nonrelativistic pion loops is typically $1/(4\pi)$, rather than $1/(16\pi^2)$ [6]. Therefore, the $\pi\Lambda_c^*$ propagation generally contributes a

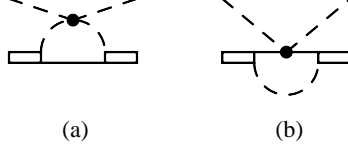


FIG. 3: Subleading $\pi\Lambda_c^*$ potentials.

factor of $Q/4\pi$.

The once-iterated potential, the second diagram in the second line of Fig. 2, scales as

$$\frac{m_\pi^3}{f_\pi^2 Q^2} \frac{Q}{4\pi} \frac{m_\pi^3}{f_\pi^2 Q^2} \sim \frac{m_\pi^3}{f_\pi^2 Q^2} \frac{Q}{\epsilon m_\pi} \quad (5)$$

Because $Q/\epsilon m_\pi \sim 1$, the once-iterated potential contributes about the same as the Born term does. By induction, we conclude that it is necessary to resum all the diagrams in the second line of Fig. 2.

With the above argumentation, we are in a position to estimate theoretical uncertainties of the present analysis by counting subleading corrections that are not included at LO. In Fig. 3 (a) S -wave pion-pion vertexes contribute a factor of m_π^2/f_π^2 . With the aforementioned counting rule applied to other elements of the diagram, pion-pion interactions are found to correct the LO $\pi\Lambda_c^*$ potential by $\mathcal{O}(\epsilon^2)$.

The Weinberg-Tomozawa term for the Σ_c provides corrections to both the Λ_c^* self energy and the $\pi\Lambda_c^*$ potential. The diagram of Fig. 3 (b) shows its correction to the potential, but it turns out to vanish after the isospin indexes are contracted. Even if it did not, its contribution would be $\mathcal{O}(\epsilon^2)$, based on power counting. The correction to the Λ_c^* self energy was found in Ref. [6] to be $\mathcal{O}(\epsilon^2)$.

Σ_c and Λ_c^* have respectively a spin-3/2 neighboring state, $\Sigma_c(2520)$ and $\Lambda_c^+(2625)$. These neighboring states are degenerate in the heavy quark limit. If we only search for possible resonances with $I(J^P) = 1(\frac{1}{2}^+)$, these spin-3/2 partners will not interfere very much despite the relatively small mass difference. For example, consider the u -channel exchange between Λ_c^* and π by a $\Sigma_c(2520)$, denoted by Σ_c^* . The $\pi\Sigma_c^*\Lambda_c^*$ transition vertex is proportional to the pion momentum square [5]. After being projected onto the S -wave, the Σ_c^* exchange is suppressed by $\mathcal{O}(\epsilon^2 Q^2/M_{hi}^2)$, where M_{hi} is the break-down scale of this specialized, two-flavor ChPT.

Let us proceed to more quantitative analyses. With $T(\vec{q}; E, E_\Lambda, q_0)$ representing the $\pi\Lambda_c^*$

amplitude, the first line of Fig. 2 translates into the following integral equation,

$$\begin{aligned}
T(\vec{q}; E, E_\Lambda, q_0) = & -\frac{h^2 m_\pi^2}{3f_\pi^2(E_\Lambda - q_0 + i0)} \\
& + i h^2 \frac{m_\pi^2}{3f_\pi^2} \int \frac{d^4 l}{(2\pi)^4} \frac{1}{E - q_0 - l_0 + i0} \frac{1}{2m_\pi l_0 - \vec{l}^2 + i0} \\
& \times \frac{T(\vec{l}; E, E_\Lambda, l_0)}{E - l_0 - \delta - \epsilon h^2 \sqrt{-2(E - l_0)m_\pi - i0} + i0},
\end{aligned} \tag{6}$$

where l_0^2 has been dropped off in the pion propagator, since $l_0 \sim \vec{l}^2/2m_\pi$. Integrating over l_0 and the angular part of \vec{l} , setting $q_0 = \vec{q}^2/2m_\pi$ to define $t(q; \mathcal{E}, \mathcal{B}) \equiv T(\vec{q}; E, E_\Lambda, q^2/2m_\pi)$, we arrive at

$$\begin{aligned}
t(q; \mathcal{E}, \mathcal{B}) = & \frac{8\pi/|r|}{3(q^2 + \mathcal{B})} + \frac{2}{3\pi} \int_{\Sigma_l} dl \frac{l^2}{q^2 - \mathcal{E} + l^2 + i0} \\
& \times \frac{t(l; \mathcal{E}, \mathcal{B})}{-\frac{1}{a} - \frac{|r|}{2}(\mathcal{E} - l^2) + \sqrt{l^2 - \mathcal{E} - i0} - i0},
\end{aligned} \tag{7}$$

where $\mathcal{E} \equiv 2m_\pi E$, $\mathcal{B} \equiv -2m_\pi E_\Lambda$, and the $\pi\Sigma_c$ scattering length and effective range have been used to make the notation more compact. The subscript Σ_l serves to remind that in order to continue $t(q; \mathcal{E}, \mathcal{B})$ to the complex \mathcal{E} plane, we need to deform the integration contour away from the positive real axis. Since we are only interested in extracting the pole position, the field renormalization constants of π and Ψ are not accounted for.

The integral in Eq. (7) actually converges. To see this, note that the q dependence on the right hand side suggests that when $q \rightarrow \infty$, $t(q; \mathcal{E}, \mathcal{B})$ vanishes as fast as q^{-2} . The convergence is also confirmed numerically. It is rather important that the pole position extracted is independent of the way the integral is regularized, for we can then state with confidence that the sought-after hadronic structure does not come out of modeling short-range QCD physics.

When searching for the poles of $t(q; \mathcal{E}, \mathcal{B})$ as a function of \mathcal{E} , we can assign any values to q^2 and \mathcal{B} , so long as the Σ_c pole of the driving term in Eq. (7) is avoided, i.e., $q^2 + \mathcal{B} \neq 0$. For definitiveness, I use $q^2 = \mathcal{E} + \mathcal{B}$, which corresponds to on-shell external pions. But this does not fix the values for both q^2 and \mathcal{B} . We will see later another choice to be made upon \mathcal{B} to make our life easier.

The main technical challenge of the work is to continue analytically the above integral equation into the complex \mathcal{E} plane. The key is to deform tactfully the integration contour so that, as \mathcal{E} moves into its second sheet, it does not interfere any singularities of the integrand.

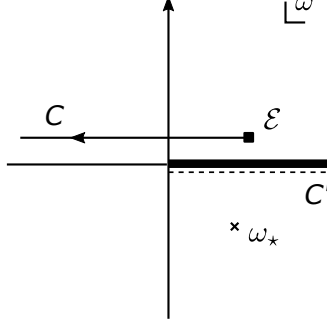


FIG. 4: The integration contour C and singularities of the integrand in the ω -plane, when \mathcal{E} is in its *first* sheet. The thick line is Singularity (1), the dashed line C' Singularity (2), and the cross Singularity (3) (see the text for detailed explanation).

It proves convenient to illustrate the contour with $\omega_l \equiv \mathcal{E} - l^2$, instead of l . Shown in Fig. 4, as \mathcal{E} approaches the real axis from above, the contour C starts at \mathcal{E} and extends leftward to infinity. Once the contour C is chosen, we can solve numerically for $t(\omega_q; \mathcal{E}, \mathcal{B})$, with $\omega_q \equiv \mathcal{E} - q^2$ also running along C .

The singularities of the integrand in Eq. (7) as a function of ω_l include the branch cut of the square root, the poles of two propagators, and possible singularities of $t(\omega_l; \mathcal{E}, \mathcal{B})$ as a function of ω_l . Excluding for the moment $t(\omega_l; \mathcal{E}, \mathcal{B})$, let us take stock of the rest of ω_l singularities:

1. The branch cut given by $\sqrt{l^2 - \mathcal{E}} = \sqrt{-\omega_l}$, shown in Fig. 4 as the thick line that runs along the positive real axis.
2. For each and every ω_q on C , there is a ω_l pole of the pion propagator $(q^2 - \mathcal{E} + l^2)^{-1} = (\mathcal{E} - \omega_l - \omega_q)^{-1}$. The whole set of these ω_l poles make up a line, represented by C' in Fig. 4. Note that C and C' are symmetric about $\omega = \mathcal{E}/2$. If the two lines do not intersect each other, the denominator of $(\mathcal{E} - \omega_l - \omega_q)^{-1}$ does not vanish for any ω_l or ω_q .
3. The pole of the dressed Λ_c^* propagator, $\omega_*(a, r)$, represented by the cross in Fig. 4.

As the starting point of C , \mathcal{E} , moves downward and crosses the real axis, the second sheet of \mathcal{E} is defined. But C must deform continuously in such a way that it does not cross or intersect any singularities listed above. Figure 5 illustrates one way to achieve this.

- First, we are free to bend the cut line of $\sqrt{-\omega_l}$ (thick line in Fig. 5) so that it accommodates the downward motion of \mathcal{E} .

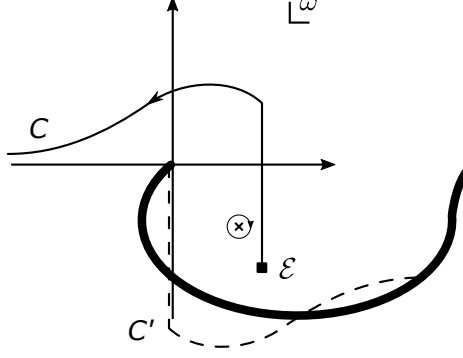


FIG. 5: The deformed integration contour C when \mathcal{E} moves into its *second* sheet. The symbols are the same as in Fig. 4, but the label ω_* is omitted to avoid clustering of symbols.

- Second, C always circumvents counterclockwise the origin from above so that C and C' do not intersect each other.
- Third, C must not cross through ω_* . But when $\mathcal{E} = \omega_*$, the contour can in no way avoid ω_* , for its starting point sits on ω_* . This so-called end-point singularity of $t(\omega_q; \mathcal{E}, \mathcal{B})$, as a function of \mathcal{E} , is the branch point that marks the $\pi\Lambda_c^*$ threshold, and the cut line is chosen conventionally to run horizontally to $+\infty$. To reflect this choice of cut line, we let C circumvent clockwise ω_* , when \mathcal{E} is to the southeast of ω_* , i.e., $\text{Re}(\mathcal{E} - \omega_*) < 0$ and $\text{Im}(\mathcal{E} - \omega_*) < 0$. This can be implemented by adding to the contour a clockwise infinitesimal circle around ω_* .

Now back to the singularities of $t(\omega_l; \mathcal{E}, \mathcal{B})$ as a function of ω_l . Inspecting the q dependence of the right hand side of Eq. (7), we find that the driving term $\propto (q^2 + \mathcal{B})^{-1}$ contributes a pole at $\omega_q = \mathcal{E} + \mathcal{B}$ to $t(\omega_q; \mathcal{E}, \mathcal{B})$ as a function of ω_q . Therefore, the contour C must not cross $(\mathcal{E} + \mathcal{B})$. On the other hand, it is at our disposal to choose the value for \mathcal{B} . The non-crossing requirement is most conveniently met by letting \mathcal{B} have negative values for both real and imaginary parts: $\text{Re}\mathcal{B} < 0$ and $\text{Im}\mathcal{B} < 0$.

The other important singularity of $t(\omega_q; \mathcal{E}, \mathcal{B})$ as a function of ω_q stems from the Σ_c propagator of the integrand $(q^2 - \mathcal{E} + l^2)^{-1} = (\mathcal{E} - \omega_l - \omega_q)^{-1}$. For ω_l always starts at $\omega_l = \mathcal{E}$, $\omega_q = 0$ is an end-point singularity of $t(\omega_q; \mathcal{E}, \mathcal{B})$ as a function of ω_q , more precisely, a branch point. The associated cut line is defined by the values of ω_q that take the Σ_c propagator on-shell: $\omega_q^{\text{cut}} = \mathcal{E} - \omega_l$. Since ω_l runs along C , it follows that the cut line of $t(\omega_q; \mathcal{E}, \mathcal{B})$ is exactly C' , the line that is symmetric with C about $\mathcal{E}/2$. And the contour C must not

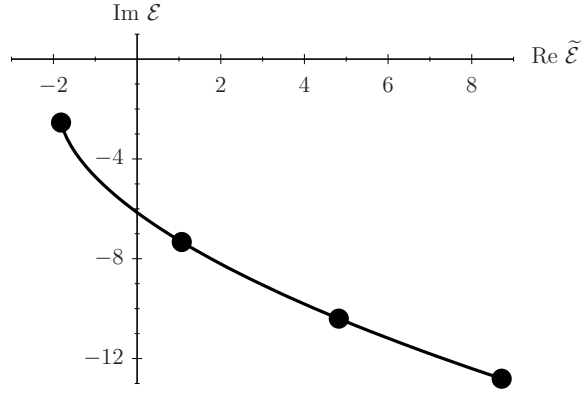


FIG. 6: As $\tilde{\delta}$ changes, the pole trajectory of the $\Sigma(\pi\pi\Sigma_c, \frac{1}{2})$. From left to right, the filled circles correspond to $\tilde{\delta} = -1, -2, -3, -4$, respectively. (See the text for more detailed definitions of $\tilde{\mathcal{E}}$ and $\tilde{\delta}$.)

insect C' because we have just established that C' is a branch cut of $t(\omega_l; \mathcal{E}, \mathcal{B})$ as a function of ω_l . But we had already made sure of that. Therefore, the contour C in Fig. 5 will do just fine even with the singularities of $t(\omega_l; \mathcal{E}, \mathcal{B})$ taken into account, provided that both real and imaginary parts of \mathcal{B} are negative.

Numerical calculations indeed indicate that there exists a resonance state with $I(J^P) = 1(\frac{1}{2}^+)$, situated near the $\pi\pi\Sigma_c$ threshold. I denote this state by $\Sigma(\pi\pi\Sigma_c, \frac{1}{2})$ in the present paper. Its existence is manifested by the resonance pole of $\pi\Lambda_c^* \rightarrow \pi\Lambda_c^*$ amplitude. A mathematically compact way to present the pole position is to define dimensionless quantities

$$\tilde{\mathcal{E}} \equiv \mathcal{E}/(\epsilon h^2 m_\pi)^2, \quad \tilde{\delta} \equiv \delta/(\epsilon^2 h^4 m_\pi), \quad (8)$$

and to show how the pole position in the $\tilde{\mathcal{E}}$ plane varies with $\tilde{\delta}$,

$$\tilde{\mathcal{E}}_{\text{pole}} = \tilde{\mathcal{E}}_{\text{pole}}(\tilde{\delta}).$$

Figure 6 shows the pole trajectory as $\tilde{\delta}$ varies from -4 to -1 .

Because Λ_c^* is only a couple of MeVs away from the $\pi\Sigma_c$ threshold, its properties h^2 and δ , determined from the pionic decay data, are sensitive to the mass splitting between π^0 and π^\pm . Before a more accurate calculation is carried out [7], we can have a flavor of the pole position of $\Sigma(\pi\pi\Sigma_c, \frac{1}{2})$ by applying two sets of parameters to the present isospin-invariant calculation, with the isospin-averaged pion and Σ_c masses adopted, $m_\pi = 138.0$ MeV and

$M_{\Sigma_c} - M_{\Lambda_c^+} = 167.1 \text{ MeV}$. One has a higher Λ_c^* mass [8]:

$$M_{\Lambda_c^*} - M_{\Lambda_c^+} = 308.7 \text{ MeV}, \quad h^2 = \frac{3}{2} \times 0.30, \quad (9)$$

which gives $\Sigma(\pi\pi\Sigma_c, \frac{1}{2})$ the following pole position,

$$M_{\Sigma(\pi\pi\Sigma_c, \frac{1}{2})} - (M_{\Sigma_c} + 2m_\pi) = (4.00 - 5.72i) \text{ MeV}. \quad (10)$$

The other is from Ref. [9]:

$$M_{\Lambda_c^*} - M_{\Lambda_c^+} = 305.8 \text{ MeV}, \quad h^2 = \frac{3}{2} \times 0.36, \quad (11)$$

resulting in the pole being situated slightly below the $\pi\pi\Sigma_c$ threshold,

$$M_{\Sigma(\pi\pi\Sigma_c, \frac{1}{2})} - (M_{\Sigma_c} + 2m_\pi) = (-0.45 - 0.02i) \text{ MeV}. \quad (12)$$

How close the $\Sigma(\pi\pi\Sigma_c, \frac{1}{2})$ pole is to the $\pi\pi\Sigma_c$ threshold is sensitive to the values of h^2 and δ , but it should not affect as much the phenomenology of more realistic decay modes $\Lambda_c^+\pi\pi\pi$ and $\Lambda_c^+\pi\pi$, as opposed to $\Sigma_c\pi\pi$. This is because the threshold of, say, $\Lambda_c^+\pi\pi\pi$ is $\simeq 30 \text{ MeV}$ lower than $\Sigma(\pi\pi\Sigma_c, \frac{1}{2})$, much larger than the uncertainty of its pole position.

If we replace Σ_c and Λ_c^* with their spin-3/2 partners, $\Sigma_c(2520)$ and $\Lambda_c^+(2625)$, and repeat the above analysis, it is likely to find the spin-3/2 partner of the $\Sigma(\pi\pi\Sigma_c, \frac{1}{2})$, with a mass a few tens of MeVs heavier. If this turns to be the case, it is conceivable to identify the pair with the lower broad peak, labeled by $\Lambda_c^+(2765)$ in Ref. [1], and observed by CLEO in decays into $\Lambda_c^+\pi^-\pi^+$ [10] where it was not ruled out that the peak could be two overlapping states. Studies based on quark models related to $\Lambda_c^+(2765)$ can be found in, for examples, Refs. [11, 12].

While a more careful confrontation with the invariant mass spectrum data is underway [7] to determine whether $\Lambda_c^+(2765)$ is indeed $\Sigma(\pi\pi\Sigma_c, \frac{1}{2})$ or the overlapping of $\Sigma(\pi\pi\Sigma_c, \frac{1}{2})$ and its spin-3/2 partner, I point out here that the decay of $\Sigma(\pi\pi\Sigma_c, \frac{1}{2})$ into $\Lambda_c^+\pi^-\pi^+$ is possible, with the dominant contribution illustrated in Fig. 7. From left to right, the first solid line represents a Σ_c intermediate state that is above its energy shell by about $2m_\pi$. After emitting a pion, the Σ_c could become on-shell, either remaining to be itself or turning into $\Sigma_c(2520)$. Then the Σ_c or $\Sigma_c(2520)$ decays into $\Lambda_c^+\pi$. This decay mechanism is consistent with the finding of Ref. [10] that $\Lambda_c^+(2765)$ appears to resonate through Σ_c and probably also Σ_c^* .

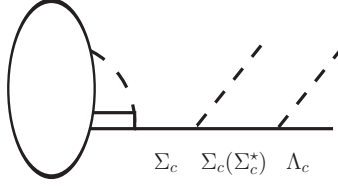


FIG. 7: The decay of $\Sigma(\pi\pi\Sigma_c, \frac{1}{2})$ into $\Lambda_c^+ \pi^- \pi^+$. The blob represents the composite structure of $\Sigma(\pi\pi\Sigma_c, \frac{1}{2})$. The symbols are the same as in Fig. 1, except for those solid-line states labeled explicitly otherwise.

Acknowledgments

I thank Fei Huang for useful discussions about the analytic continuation technique used in Ref. [13] and Songlin Lv for finding the relation between h and h_2 in the Lagrangian (1). Also acknowledged is the hospitality of the nuclear theory group at BeiHang University where part of the work was done. This work was supported in part by the National Natural Science Foundation of China (NSFC) under Grant No. 11375120.

-
- [1] K. A. Olive *et al.* [Particle Data Group Collaboration], Chin. Phys. C **38**, 090001 (2014).
 - [2] M. B. Wise, Phys. Rev. D **45**, no. 7, R2188 (1992).
 - [3] G. Burdman and J. F. Donoghue, Phys. Lett. B **280**, 287 (1992).
 - [4] T. M. Yan, H. Y. Cheng, C. Y. Cheung, G. L. Lin, Y. C. Lin and H. L. Yu, Phys. Rev. D **46**, 1148 (1992) Erratum: [Phys. Rev. D **55**, 5851 (1997)].
 - [5] P. L. Cho, Phys. Rev. D **50**, 3295 (1994) [hep-ph/9401276].
 - [6] Bingwei Long, Phys. Rev. D **94**, no. 1, 011503 (2016), [arXiv:1508.06084 [hep-ph]].
 - [7] Songlin Lv and Bingwei Long, in preparation.
 - [8] G. Chiladze and A. F. Falk, Phys. Rev. D **56**, R6738 (1997) [hep-ph/9707507].
 - [9] T. Aaltonen *et al.* [CDF Collaboration], Phys. Rev. D **84**, 012003 (2011) [arXiv:1105.5995 [hep-ex]].
 - [10] M. Artuso *et al.* [CLEO Collaboration], Phys. Rev. Lett. **86**, 4479 (2001) [hep-ex/0010080].
 - [11] S. Capstick and N. Isgur, Phys. Rev. D **34**, 2809 (1986).
 - [12] L. A. Copley, N. Isgur, and G. Karl, Phys. Rev. D **20**, 768 (1979); Erratum: [Phys. Rev. D

23, 817 (1981)].

- [13] M. Doring, C. Hanhart, F. Huang, S. Krewald and U.-G. Meissner, Nucl. Phys. A **829**, 170 (2009) [arXiv:0903.4337 [nucl-th]].